

# Gamow shell model and realistic nucleon-nucleon interactions

G. Hagen,<sup>1,2</sup> M. Hjorth-Jensen,<sup>3</sup> and N. Michel<sup>1,2</sup>

<sup>1</sup>*Department of Physics and Astronomy, University of Tennessee, Knoxville, Tennessee 37996, U.S.A.*

<sup>2</sup>*Physics Division, Oak Ridge National Laboratory, P.O. Box 2008, Oak Ridge, TN 37831, U.S.A.*

<sup>3</sup>*Department of Physics and Center of Mathematics for Applications, University of Oslo, N-0316 Oslo, Norway*

(Dated: November 3, 2018)

We present a new and efficient method to obtain a Gamow shell-model basis and matrix elements generated by realistic nucleon-nucleon interactions. We derive a self-consistent Hartree-Fock potential from the renormalized  $N^3$ LO interaction model. The corresponding Gamow one-body eigenstates are generated in a plane wave basis in order to build a Gamow shell-model set of basis states for the closed shell nuclei  ${}^4\text{He}$  and  ${}^{16}\text{O}$ . We address also the problem of representing a realistic nucleon-nucleon interaction in a two-particle Berggren basis in the laboratory frame. To achieve this, an expansion of matrix elements of the residual nucleon-nucleon interaction in a finite set of harmonic oscillator wave functions is used. We show that all loosely bound and narrow resonant states converge surprisingly fast. Even broad resonances in these two-particle valence systems converge within a reasonable number of harmonic oscillator functions. Examples of  ${}^6\text{He}$  and  ${}^{18}\text{O}$  Gamow shell-model calculations using  ${}^4\text{He}$  and  ${}^{16}\text{O}$  as closed shell cores are presented. This procedure allows Gamow shell-model calculations to be performed with all realistic nucleon-nucleon interactions and with either momentum or position space representations for the Gamow basis. Perspectives for nuclear structure calculations of dripline nuclei are outlined.

PACS numbers: 21.60.Cs, 21.10.-k, 24.10.Cn, 24.30.Gd

## I. INTRODUCTION

A challenge in modern nuclear physics is the description of nuclei far from the valley of stability. These nuclei exhibit unusual features such as very low particle-emission thresholds, halo densities and unbound ground states. A proper understanding of the mechanisms underlying the formation of such nuclei is presently a great challenge to nuclear theory, especially the case of two-neutron Borromean halos such as  ${}^6\text{He}$  and  ${}^{11}\text{Li}$ . The theoretical description of such exotic nuclei cannot be worked out within standard models because of the appearance of strong couplings to the continuum.

The extreme clusterization of Borromean nuclei into an ordinary core nucleus and a veil of halo nucleons has motivated few-body approaches such as the hyperspherical harmonic method and momentum space Faddeev equations to these nuclei [1]. However, the few-body modeling of Borromean and halo nuclei is not completely satisfying as the treatment of core excitations and the anti-symmetrization between core and valence nucleons is therein approximate.

An *ab initio* description of these nuclei, taking into account all relevant degrees of freedom, would alleviate the defects of such cluster approaches. To achieve this, a reformulation of the shell model using a single-particle basis of bound, resonant and scattering states appears to be the most straightforward method. The Continuum shell model [2, 3, 4, 5, 6] and the recently developed shell model embedded in the continuum (SMEC) [7, 8, 9, 10] offer such a possibility. In SMEC, two subspaces of bound/quasi-bound states and scattering states are introduced and their coupling taken into account following the techniques discussed in for example Ref. [5, 6]. However, most calculations have been performed with only one-particle decay channels. While the theoretical formulation of SMEC with two-particle decay channels has been formulated (see Ref. [10] with applications to two-proton radioactivity), exact three-body asymptotics have never been applied numerically. The very rapidly increasing complexity of SMEC with many-body decay channels is a hindrance to the study of cluster-emitting systems, such as in particular Borromean nuclei.

The newly developed Gamow shell model [11, 12, 13, 14, 15, 16, 17, 18, 19, 20] has proven to be a reliable tool in order to probe the structure of such nuclei. This model unifies structure and reaction properties of nuclei, and most importantly allows for an exact treatment of antisymmetry and has no limitation on the number of particles in the continuum. It is then particularly well suited for the study of Borromean nuclei. The starting point of the Gamow shell model is the Berggren completeness relation, where bound, resonant and scattering states are treated on an equal footing [21, 22, 23, 24, 25]. The completeness relation is built upon bound, resonant states and an integral over a continuum of scattering states with complex energy. This integral has to be discretized in order to be applied in numerical calculations. A complete many-body Berggren basis is then constructed with Slater determinants integrating bound, resonant and non-resonant discretized continuum orbitals. The Gamow shell model can be seen as a direct generalization of the standard shell model, where the standard harmonic oscillator set of states is replaced by a Gamow basis.

An important question concerns the choice of the potential to generate the one-body Gamow basis states. In Gamow shell-model calculations, the single-particle basis has normally been constructed from a Woods-Saxon or a Gaussian potential depicting  ${}^4\text{He}$  or  ${}^{16}\text{O}$  cores, fitted to reproduce the single-particle states of  ${}^5\text{He}$  and  ${}^{17}\text{O}$ , respectively [11, 20]. However, in a fully microscopic approach, the single-particle basis should be constructed from the free nucleon-nucleon interaction or more complicated three and/or many-body interactions. This can be done by summing various diagrams in many-body perturbation theory. At lowest order this approach is given by the Hartree-Fock approximation (see Ref. [11] where a Gamow-Hartree-Fock basis was derived and applied to schematic interactions.)

In many-body perturbation theory, one cannot use the free nucleon-nucleon interaction, since it yields strongly repulsive and/or diverging matrix elements at short internucleonic distances. In order to remove these divergencies, renormalized nucleon-nucleon interactions have been constructed from the Brueckner G-matrix approach [26, 27, 28]. The G-matrix is a soft interaction, which is obtained by resumming in-medium particle-particle correlations.

Recently, an alternative renormalization scheme which integrates out the high momentum components of the nucleon-nucleon interactions has been proposed [29, 30, 31, 32, 33]. Using a similarity transformation of the two-nucleon Hamiltonian, a Hermitian soft-core effective nucleon-nucleon interaction is obtained in a model space defined by a cutoff  $\Lambda$  in the relative momentum between the nucleons. This renormalized interaction has become known as a low-momentum nucleon-nucleon interaction, labeled  $V_{\text{low}-k}$ . The interaction  $V_{\text{low}-k}$  is an energy and nucleus independent effective interaction which reproduces nucleon-nucleon scattering data, but displays a sizeable dependence on  $\Lambda$ .

In this work, the single-particle Gamow Hartree-Fock basis is constructed using a renormalized interaction of the  $V_{\text{low}-k}$  type, derived by similarity transformation techniques of the nucleon-nucleon interaction. Our renormalization scheme requires a plane wave basis formulation of the Schrödinger equation. Such a basis is a natural starting point since nucleon-nucleon interactions are usually derived explicitly in momentum space, as for example the  $\text{N}^3\text{LO}$  interaction [34, 35]. In order to perform Gamow Hartree-Fock calculations, the nucleon-nucleon interaction has to be defined by the coordinates of the laboratory system. The transformation of the interaction from the relative and center of mass frame to the laboratory frame is performed with the so-called vector brackets [27, 36, 37, 38]. These are the less known momentum space analogs of the Moshinsky transformation coefficients of the harmonic oscillator representation, generalizing the Talmi transformation to arbitrary bases. In the presence of unbound states such as in a Gamow basis, the single-particle potential has to be analytically continued in the complex  $k$ -plane. In Ref. [19], it was shown how a single-particle Berggren basis can be obtained by the contour deformation method in a basis of spherical Bessel functions.

For a microscopic approach to be fully consistent, the realistic nucleon-nucleon interaction should generate both a single-particle basis through Hartree-Fock calculations and an effective nucleon-nucleon interaction to be diagonalized in the Gamow shell model. We can obtain this by letting the renormalized nucleon-nucleon interaction to be expressed in a two-particle Berggren basis. However, the difficulty in analytically continuing the vector transformation coefficients to the complex  $k$ -space, prevents such a derivation. In this work, an alternative approach to calculate realistic interactions in Gamow bases is proposed. The method is based on an expansion of the nucleon-nucleon interaction in a finite set of harmonic oscillator wave functions. Within this framework, the analytic continuation of the nuclear interaction is trivial, and matrix elements can therein be very efficiently calculated through the use of the standard Talmi transformation. As will be shown, this method provides well converged energies and wave functions in the Gamow shell-model calculations with a small number of harmonic oscillator states. In addition, as harmonic oscillator wave functions have a similar behavior in momentum and position space, both momentum space and coordinate space representations can be used for the Gamow basis. This method may also provide a solution to the problem of spurious center of mass motion in Gamow shell-model calculations.

The outline of the paper is as follows. In Sec. II, the derivation of a renormalized nucleon-nucleon interaction suitable for a perturbative many-body approach in the Gamow shell model is described. In Sec. III, the self-energy and Gamow Hartree-Fock single-particle basis of the  $V_{\text{low}-k}$  interaction are constructed and applied to the  ${}^4\text{He}$  and  ${}^{16}\text{O}$  closed-shell nuclei. Sec. IV outlines the harmonic oscillator expansion method for the nucleon-nucleon interaction, and Sec. V illustrates applications in Gamow shell-model calculations for two selected valence systems,  ${}^6\text{He}$  and  ${}^{18}\text{O}$ . There we discuss also the convergence of narrow and broad resonances as functions of the number of harmonic oscillator wave functions used in the expansion. Sec. VI points out the equivalence between the momentum and the position space formulations of the Gamow shell model when the harmonic oscillator expansion method is used. Finally, in Sec. VII we outline our conclusions and future perspectives.

## II. RENORMALIZED NUCLEON-NUCLEON INTERACTION

In order to build the Gamow Hartree-Fock potential in  $k$ -space and a Gamow shell-model Hamiltonian matrix, it is necessary to construct the self-energy  $\Sigma(k_a l_a j_a, k_b)$  defined by the inclusion of various diagrams in many-body

perturbation theory, discussed in Sec. III. Note here and in the following discussion the distinction between  $k_a, k_b$  and  $k$  and  $l_a$  and  $l$ . The notations  $k_a$  or  $l_a$  (latin letters) refer to the quantum numbers of a single-particle state  $a$ , whereas  $l$  or  $k$  without subscripts (or with greek letters as subscripts) refer to the coordinates of the relative motion.

To compute many-body perturbation diagrams, the nucleon-nucleon interaction has to enter a perturbative treatment. Hence, the free nucleon-nucleon interaction, giving rise to diverging matrix elements, cannot be used directly and has to be renormalized. Since parts of our formalism is based on computing the self-energy in a momentum basis, it is convenient here to use a renormalization scheme based on a cutoff in momentum space as discussed by Bogner *et al* [29] and Fujii *et al* [30, 31].

This approach is based on two steps, a diagonalization in momentum space for relative momenta  $k \in [0, \infty)$  of the two-body Schrödinger equation and a similarity transformation [30, 31] to relative momenta  $k \in [0, \Lambda]$ ,  $\Lambda$  defining the relative momenta model space. Typical values of  $\Lambda$  are in the range of  $\sim 2 \text{ fm}^{-1}$ . The nucleon-nucleon interaction is diagonal in the center of mass motion. One can therefore easily map the full diagonalization problem onto a smaller space via a similarity transformation and obtain thereby an effective interaction for a model space defined for low momenta. This interaction has been dubbed  $V_{\text{low-}k}$  in the literature, see for example Ref. [29]. The effective low-momentum interaction  $V_{\text{low-}k}$  is constructed in such a way that it reproduces exactly the main characteristics of the nucleon-nucleon wave function in the full space.

The interaction  $V_{\text{low-}k}$  looks attractive at first glance, but may generate undesirable features in the Gamow shell model. Many-body calculations using a renormalized nucleon-nucleon interaction of the low-momentum type introduce a strong dependence on the cutoff  $\Lambda$  in momentum space. By integrating out high momentum modes of the nucleon-nucleon interaction, one excludes certain intermediate excitations in the many-body problem. While the two-body problem is exact with  $V_{\text{low-}k}$ , the three-body problem will not be. In Ref. [33]  $V_{\text{low-}k}$  was accompanied with a  $\Lambda$ -dependent three-body force in order to reproduce the ground-state energies of  ${}^4\text{He}$  and  ${}^3\text{H}$  for each value of  $\Lambda$ . It is hoped that a three-body force is sufficient to eliminate the  $\Lambda$  dependence for heavier nuclei. However, if it turns out that one needs to go beyond three-body forces for nuclei with  $A > 4$ , many-body calculations starting with  $V_{\text{low-}k}$  are futile.

Alternatively, one could have defined a so-called  $G$ -matrix in momentum space as effective interaction [26, 27, 28, 39]. The latter introduces a dependence on the chosen starting energy and a reference to a given Fermi energy. This dependence can be eliminated by introducing for example higher-order terms in many-body perturbation theory [39]. We relegate such a discussion to future work. It must be stressed that the aim here is to demonstrate the feasibility of obtaining a single-particle basis for Gamow shell-model calculations using a realistic interaction. We adopt therefore a pragmatic approach and use  $V_{\text{low-}k}$  simply because it is easier to implement numerically in order to renormalize the nucleon-nucleon interaction.

In the following we outline the procedure to obtain a Hermitian interaction  $V_{\text{low-}k}$  based on the similarity transformation discussed in Refs. [30, 31, 40, 41]. A unitary transformation can be parametrized in terms of the model space  $P$  and the excluded space  $Q$  via

$$U = \begin{pmatrix} P(1 + \omega^\dagger \omega)^{-1/2} P & -P\omega^\dagger(1 + \omega\omega^\dagger)^{-1/2} Q \\ Q\omega(1 + \omega^\dagger \omega)^{-1/2} P & Q(1 + \omega\omega^\dagger)^{-1/2} Q \end{pmatrix}, \quad (1)$$

where the wave operator  $\omega$  is defined to satisfy the condition

$$\omega = Q\omega P, \quad (2)$$

the so-called decoupling condition [42]. Note that the unitary transformation is by no means unique. In fact, one can construct infinitely many different unitary transformations which decouple the  $P$  and the  $Q$  subspaces, as discussed by Kuo *et al* [43]. The above transformation depends only on the operator  $\omega$  which mixes the  $P$  and  $Q$  subspaces and is in some sense “the minimal possible” unitary transformation. Following the method of Ref. [30], one obtains

$$U = (1 + \omega - \omega^\dagger)(1 + \omega\omega^\dagger + \omega^\dagger\omega)^{-1/2}. \quad (3)$$

The above operator  $U$  leads to the effective interaction  $\tilde{V}$  using the definition

$$\tilde{V} = U^{-1}(T + V)U - T, \quad (4)$$

where  $T$  is the kinetic energy of the nucleons and  $V$  is the free nucleon-nucleon interaction.

To express the renormalized interaction in momentum space, one starts with the Schrödinger equation for the relative momentum  $k$ ,

$$\int dk' k'^2 \langle k|T + V|k'\rangle \langle k'|\psi_\alpha\rangle = E_\alpha \langle k|\psi_\alpha\rangle, \quad (5)$$

where the plane wave states are eigenfunctions of the kinetic energy operator  $T$  in the relative system and form a complete set

$$\int dk k^2 |k\rangle \langle k| = \mathbb{1}. \quad (6)$$

The momentum space Schrödinger equation is solved as a matrix equation by discretizing the integration interval by some suitable rule, (here, the Gauss-Legendre quadrature is used). The discretized Schrödinger equation reads

$$\sum_{\gamma} w_{\gamma} k_{\gamma}^2 \langle k_{\delta} | T + V | k_{\gamma} \rangle \langle k_{\gamma} | \psi_{\alpha} \rangle = E_{\alpha} \langle k_{\delta} | \psi_{\alpha} \rangle, \quad (7)$$

where  $k_{\gamma}$  are the integration points and  $w_{\gamma}$  the corresponding quadrature weights. Introducing  $|\bar{k}_{\delta}\rangle = k_{\delta} \sqrt{w_{\delta}} |k_{\delta}\rangle$ , Eq. (7) becomes

$$\sum_{\gamma} \langle \bar{k}_{\delta} | T + V | \bar{k}_{\gamma} \rangle \langle \bar{k}_{\gamma} | \psi_{\alpha} \rangle = E_{\alpha} \langle \bar{k}_{\delta} | \psi_{\alpha} \rangle, \quad (8)$$

where

$$\sum_{\delta=1}^N |\bar{k}_{\delta}\rangle \langle \bar{k}_{\delta}| = \mathbb{1}, \quad \langle \bar{k}_{\delta} | \bar{k}_{\gamma} \rangle = \delta_{\delta,\gamma}. \quad (9)$$

The matrix elements of the Hamiltonian are expressed in the plane wave basis :

$$H_{\delta,\gamma} = \langle \bar{k}_{\delta} | T + V | \bar{k}_{\gamma} \rangle = \frac{k_{\delta}^2}{m} \delta_{\delta,\gamma} + \sqrt{w_{\delta} w_{\gamma}} k_{\delta} k_{\gamma} V(k_{\delta}, k_{\gamma}), \quad (10)$$

where  $m$  is the average of the proton and the neutron masses. The full space is now divided in a model space  $P$  and an orthogonal complement space  $Q$ . The model space  $P$  consists in the  $N_P$  plane wave states lying below the cutoff  $\Lambda$ , and the  $Q$ -space consists of the remaining states, viz.

$$P = \{|\bar{k}\rangle, |k| \leq \Lambda\}, \quad Q = \{|\bar{k}\rangle, \Lambda < |k| < \infty\}. \quad (11)$$

The model space is thus defined for all momenta  $k \in [0, \Lambda] \text{ fm}^{-1}$ . In order to obtain an effective interaction in the model space  $P$ , the decoupling condition in Eq. (2) has to be fulfilled. Once the transformation matrix  $\omega$  in the plane wave basis  $\langle \bar{k} | Q \omega P | \bar{k} \rangle$  is obtained, the low-momentum effective nucleon-nucleon interaction  $V_{\text{low-k}}$  reads

$$\begin{aligned} \langle \bar{k} | P V_{\text{low-k}} P | \bar{k}' \rangle &= \sum_{k''} \sum_{k'''} \langle \bar{k} | P (P + \omega^T \omega)^{1/2} P | k'' \rangle \langle k'' | P (T + V) P | k''' \rangle \langle k''' | P (P + \omega^T \omega)^{-1/2} P | \bar{k}' \rangle \\ &- \frac{k^2}{m} \delta_{kk'}, \end{aligned} \quad (12)$$

see also Ref. [30] for further details. The effective model space interaction in the original plane wave basis  $|k_{\delta}\rangle$  is then given by

$$\langle k_{\delta} | V_{\text{low-k}} | k_{\gamma} \rangle = \frac{\langle \bar{k}_{\delta} | V_{\text{low-k}} | \bar{k}_{\gamma} \rangle}{\sqrt{w_{\delta} w_{\gamma}} k_{\delta} k_{\gamma}}, \quad (13)$$

where  $\{|k_{\delta}\rangle, |k_{\gamma}\rangle\} \in P$ .

### III. DERIVATION OF SELF-CONSISTENT GAMOW HARTREE-FOCK BASIS

The renormalized nucleon-nucleon interaction  $V_{\text{low-k}}$  is defined in terms of various quantum numbers as follows

$$\langle k l K L (\mathcal{J}) S T_z | V_{\text{low-k}} | k' l' K L (\mathcal{J}) S T_z \rangle, \quad (14)$$

where the variables  $k, k'$  and  $l, l'$  denote respectively relative and angular momenta, while  $K$  and  $L$  are the quantum numbers of the center of mass motion.  $\mathcal{J}, S$  and  $T_z$  represent the total angular momentum in the relative and center of mass system, spin and isospin projections, respectively.

The  $A$ -body Hamiltonian  $H$  is defined as

$$H = \frac{1}{2m} \sum_{i=1}^A \mathbf{k}_i^2 + \sum_{i<j}^A V_{\text{low-k}}(i, j). \quad (15)$$

The spurious center of mass energy is removed by writing the internal kinetic energy as

$$T_{\text{in}} = T - T_{\text{c.m.}} = \left(1 - \frac{1}{A}\right) \sum_{i=1}^A \frac{\mathbf{k}_i^2}{2m} - \sum_{i<j}^A \frac{\mathbf{k}_i \cdot \mathbf{k}_j}{mA}. \quad (16)$$

The introduction of an additional two-body term yields a modified two-body interaction

$$H_{\text{I}} = V_{\text{low-k}} + V_{\text{c.m.}} = \sum_{i<j}^A \left( V_{\text{low-k}}(i, j) - \frac{\mathbf{k}_i \cdot \mathbf{k}_j}{mA} \right), \quad (17)$$

resulting in a total Hamiltonian given by

$$H = \left(1 - \frac{1}{A}\right) \sum_{i=1}^A \frac{\mathbf{k}_i^2}{2m} + H_{\text{I}}. \quad (18)$$

In all calculations reported in this manuscript, the modified two-body Hamiltonian defined in Eq. (17) is employed.

Starting from the renormalized momentum-space version of the nucleon-nucleon interaction  $V_{\text{low-k}}$ , with matrix elements in the relative and center of mass system, one can obtain the corresponding matrix elements in the laboratory system through appropriate transformation coefficients [36, 37, 38]. This transformation proceeds through the definition of a two-particle state in the laboratory system. With these coefficients, the expression for a two-body wave function in momentum space using the laboratory coordinates can be written as

$$\begin{aligned} |(k_a l_a j_a t_{z_a})(k_b l_b j_b t_{z_b})JT_z\rangle &= \sum_{lL\lambda S\mathcal{J}} \int k^2 dk \int K^2 dK \begin{Bmatrix} l_a & l_b & \lambda \\ \frac{1}{2} & \frac{1}{2} & S \\ j_a & j_b & J \end{Bmatrix} \\ &\times (-1)^{\lambda+\mathcal{J}-L-S} F \hat{\mathcal{J}} \hat{\lambda}^2 \hat{j}_a \hat{j}_b \hat{S} \begin{Bmatrix} L & l & \lambda \\ S & J & \mathcal{J} \end{Bmatrix} \\ &\times \langle klKL | k_a l_a k_b l_b \lambda \rangle |klKL(\mathcal{J})SJT_z\rangle, \end{aligned} \quad (19)$$

where  $\langle klKL | k_a l_a k_b l_b \lambda \rangle$  is the transformation coefficient (vector bracket) from the relative and center of mass system to the laboratory system defined in Refs. [37, 38]. The factor  $F$  is defined as  $F = (1 - (-1)^{l+S+T_z})/\sqrt{2}$  if we have identical particles only ( $T_z = \pm 1$ ) and  $F = 1$  for different particles (protons and neutrons here,  $T_z = 0$ ).

The transformation coefficient  $\langle klKL | k_a l_a k_b l_b \lambda \rangle$  is given by [36, 37, 38]

$$\langle klKL | k_a l_a k_b l_b \lambda \rangle = \frac{4\pi^2}{kK k_a k_b} \delta(w) \theta(1 - x^2) A(x), \quad (20)$$

with

$$w = k^2 + \frac{1}{4}K^2 - \frac{1}{2}(k_a^2 + k_b^2), \quad (21)$$

$$x = (k_a^2 - k^2 - \frac{1}{4}K^2)/kK, \quad (22)$$

and

$$A(x) = \frac{1}{2\lambda+1} \sum_{\mu} [Y^l(\hat{k}) \times Y^L(\hat{K})]_{\mu}^{\lambda*} \times [Y^{l_a}(\hat{k}_a) \times Y^{l_b}(\hat{k}_b)]_{\mu}^{\lambda}. \quad (23)$$

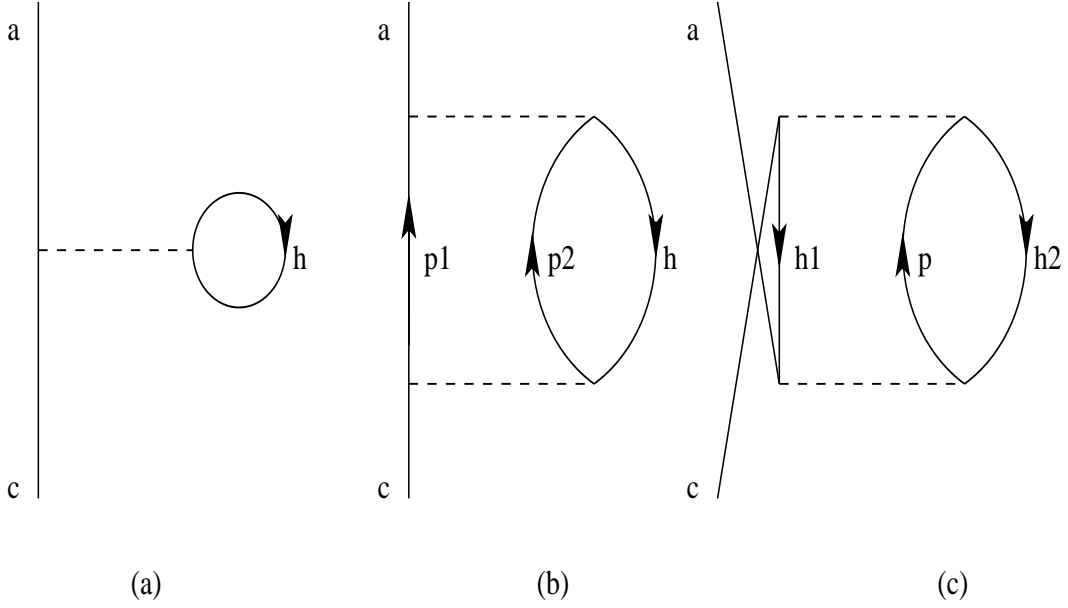


FIG. 1: Diagrams through second order of the interaction  $H_I$ . Diagram (a) is the first order Hartree-Fock term while diagrams (b) and (c) are the  $2p-1h$  and  $2h-1p$  corrections, respectively. The labels  $a$  and  $c$  represent the outgoing and incoming states, respectively. The intermediate particle states are labeled as  $p, p_1, p_2$  with upward arrows and the intermediate hole states as  $h, h_1, h_2$  with downward arrows. The dotted lines represent the interaction  $H_I$ .

The functions  $Y^l$  are the standard spherical harmonics,  $x$  is the cosine of the angle between  $\vec{k}$  and  $\vec{K}$  so that the step function takes input values from 0 to 1. In our codes, the coordinate system of Kuo *et al.* [38] was chosen.

To compute the Hartree-Fock (HF) diagram (see Fig. 1 (a)) we need matrix elements in a mixed representation of bound and scattering states such as

$$\langle (k_a l_a j_a t_{z_a})(n_b l_b j_b t_{z_b})JT_z | H_I | (k_c l_c j_c t_{z_c})(n_d l_d j_d t_{z_d})JT_z \rangle, \quad (24)$$

where the labels  $a$  and  $c$  represent scattering states and  $b$  and  $d$  represent bound states. All matrix elements discussed here are assumed to be antisymmetrized (AS). Note that the two-body center of mass correction term  $V_{c.m.}$  in Eq. (17) is calculated directly in the laboratory coordinates using the Wigner-Eckart theorem, while the renormalized nucleon-nucleon interaction is given in laboratory coordinates using the transformation given in Eq. (19). The calculation of these matrix elements requires the knowledge of two-body states in a mixed representation with for example harmonic oscillator wave functions  $R_{n_a l_a}$  representing the bound states and plane waves for the resonant or continuum states

$$|(n_a l_a j_a t_{z_a})(k_b l_b j_b t_{z_b})JT_z\rangle = \int k_a^2 dk_a R_{n_a l_a}(k_a) |(k_a l_a j_a t_{z_a})(k_b l_b j_b t_{z_b})JT_z\rangle, \quad (25)$$

where  $k_a l_a j_a$  and  $n_a l_a j_a$  are respectively plane wave and harmonic oscillator wave functions. The two-body state is represented by the quantum numbers of the total angular momentum  $J$  and isospin projection  $T_z$ .

With these matrix elements, the expression for the HF diagram shown in Fig. 1(a) can be derived

$$\mathcal{V}_{HF}(k_a k_c l_a j_a t_{z_a}) = \frac{1}{\hat{j}_a} \sum_{\hat{j}_a} \sum_J \sum_{n_h l_h j_h t_{z_h}} \hat{j}_a^2 \langle (k_a l_a j_a t_{z_a})(n_h l_h j_h t_{z_h})JT_z | H_I | (k_c l_c j_c t_{z_c})(n_h l_h j_h t_{z_h})JT_z \rangle_{AS}, \quad (26)$$

where  $\hat{x} = \sqrt{2x+1}$  and  $n_h l_h j_h t_{z_h}$  are the quantum numbers of the nucleon hole states. The variables  $l_a, j_a, t_{z_a}$  are the orbital angular momentum, total angular momentum and isospin projection ( $t_{z_a} = \pm 1/2$ ) of the incoming/outgoing nucleon, and  $k_a$  ( $k_c$ ) the outgoing (incoming) particle momenta. The mixed matrix elements of the two-body center of mass correction term needed in the HF calculation reads

$$\begin{aligned} \langle (k_a l_a j_a t_{z_a})(n_h l_h j_h t_{z_h})JT_z | -\frac{\mathbf{k}_1 \cdot \mathbf{k}_2}{mA} | (k_c l_c j_c t_{z_c})(n_h l_h j_h t_{z_h})JT_z \rangle_{AS} = \\ \frac{1}{mA} (2j_a + 1) (2j_h + 1) \begin{pmatrix} j_a & 1 & j_h \\ 1/2 & 0 & -1/2 \end{pmatrix}^2 \begin{Bmatrix} j_a & j_h & J \\ j_c & j_h & 1 \end{Bmatrix} \end{aligned}$$

$$\times \left\{ \frac{1 + (-1)^{l_a + l_h + 1}}{2} \right\} k_a k_c R_{n_h l_h}(k_a) R_{n_h l_h}(k_c) \delta_{j_a j_c} \delta_{l_a l_c} \delta_{t_{z_a} t_{z_h}} \delta_{t_{z_c} t_{z_h}}. \quad (27)$$

In summary, if we limit ourselves to the computation of the HF contribution, the expression for the self-energy reads

$$\Sigma(j_a l_a k_a k_c) = \mathcal{V}_{HF}(j_a l_a k_a k_c). \quad (28)$$

In this work, only the HF contribution is considered, while in Ref. [26] the authors also studied contributions from  $2p - 1h$  and  $2h - 1p$  intermediate states. They yield an imaginary term which can be related to its real part via a dispersion relation.

To calculate the contributions from the  $2p - 1h$  diagrams like the example displayed in Fig. 1 (b) (or similarly the  $2h - 1p$  diagram of Fig. 1 (c)) we evaluate the imaginary part first. The real part is obtained through the dispersion relations to be defined below. The analytical expression for the imaginary contribution of the  $2p - 1h$  diagram, which gives rise to an explicit energy dependence of the self-energy, is

$$\begin{aligned} \mathcal{W}_{2p-1h}(j_a l_a k_a k_c t_{z_a} \omega) &= -\frac{1}{\hat{j}_a^2} \sum_{n_h l_h j_h t_{z_h}} \sum_J \sum_{l L S \mathcal{J}} \int k^2 dk \int K^2 dK \hat{J} \hat{T} \\ &\times \langle (k_a l_a j_a t_{z_a})(n_h l_h j_h t_{z_h}) J T_z | H_I | k l K L(\mathcal{J}) S J T_z \rangle \\ &\times \langle k l K L(\mathcal{J}) S J T_z | H_I | (k_c l_a j_a t_{z_a})(n_h l_h j_h t_{z_h}) J T_z \rangle \\ &\times \pi \delta \left( \omega + \varepsilon_h - \frac{K^2}{4M_N} - \frac{k^2}{M_N} \right), \end{aligned} \quad (29)$$

where  $\omega$  is the energy of the incoming nucleon in a state  $a$ . The quantities  $klKL(\mathcal{J})SJT_z$  are the quantum numbers of the intermediate two-particle state. To compute the two-particle-one-hole diagram given by the second-order diagram of Fig. 1 (b), the following matrix elements are needed

$$\langle (k_a l_a j_a t_{z_a})(n_b l_b j_b t_{z_b}) J T_z | H_I | k l K L(\mathcal{J}) S T_z \rangle. \quad (30)$$

The contributions to the real part of the self-energy from Eq. (29) can be obtained through the following dispersion relation

$$\mathcal{V}_{2p-1h}(j_a l_a k_a k_c t_{z_a} \omega) = \frac{P}{\pi} \int_{-\infty}^{\infty} \frac{\mathcal{W}_{2p-1h}(j_a l_a k_a k_c t_{z_a} \omega')}{\omega' - \omega} d\omega', \quad (31)$$

where  $P$  takes the principal value of the integral. Since  $\mathcal{W}_{2p-1h}$  is different from zero only for positive values of  $\omega'$  and its diagonal matrix elements are negative, this dispersion relation implies that the diagonal elements of  $\mathcal{V}_{2p-1h}$  will be attractive for negative values of  $\omega$ . This attraction should increase for small positive energies. It will eventually decrease and become repulsive only for large positive values of the energy of the interacting nucleon. Similar expressions can also be derived for second-order diagrams with  $2h - 1p$  intermediate states [26]. Inclusion of these terms will be presented in a future work (see also the discussion in Sec. VII).

The equations above for the nucleon self-energy are only valid along the real-energy axis. However,  $\Sigma(j_a l_a k_a k_c)$  has to be analytically continued from the real  $k$ -axis to the complex  $k$ -plane in order to obtain a genuine Gamow shell-model single-particle basis. The derivation of a Berggren basis in momentum space with the Contour Deformation Method was described in Ref. [19]. The analytical continuation of  $\Sigma(j_a l_a k_a k_c)$  to the complex  $k$ -plane leads to theoretical and practical difficulties due to the appearance of Dirac and Heaviside distributions in vector brackets (see Eq. (20)). However, once the self-consistent self-energy has been obtained along the real  $k$ -axis, the HF potential can be simply continued to the complex plane via two sets of Fourier-Bessel transformations. To obtain a self-consistent HF potential in the complex  $k$ -plane, the following scheme is employed :

- The first step is to calculate  $\mathcal{V}_{HF}$  self-consistently on a grid on the real momentum axis using the interaction  $H_I$  of Eqs. (17) and (26).
- When a self-consistent solution has been obtained,  $\mathcal{V}_{HF}$  is calculated in position space via a double Fourier-Bessel transform.

$$\mathcal{V}_{HF}(j l r r') = \frac{2}{\pi} \int_0^\infty dk k^2 \int_0^\infty dk k^2 j_l(kr) j_l(k'r') \mathcal{V}_{HF}(j l k k'). \quad (32)$$

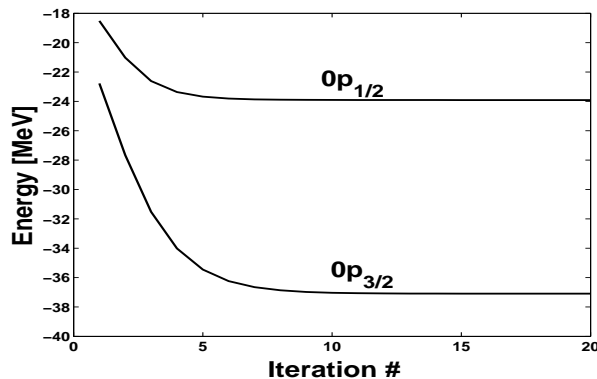


FIG. 2: Convergence of the  $0p_{3/2}$  and the  $0p_{1/2}$  energies in  $^{16}\text{O}$  with respect to iteration number in the self-consistent HF calculation. Here we used a model space  $\Lambda = 1.9\text{fm}^{-1}$  in the construction of  $V_{\text{low-}k}$ .

- Having obtained  $\mathcal{V}_{HF}$  in the  $r$ -plane we may go back to the complex  $k$ -plane using one more Fourier-Bessel transformation. On an inversion symmetric contour  $L^+$  in the complex  $k$ -plane, the HF potential becomes

$$\mathcal{V}_{HF}(jlk k') = \int_0^\infty dr r^2 \int_0^\infty dr' r'^2 j_l(kr) j_l(k'r') \mathcal{V}_{HF}(jlr r'), \quad (33)$$

where  $k$  and  $k'$  belong to the contour  $L^+$  and are therefore complex. The analytically continued single-particle Schrödinger equation on a general inversion symmetric contour then takes the form

$$\frac{\hbar^2}{m_{\text{eff}}} k^2 \psi_{nlj}(k) + \int_{L^+} dk' k'^2 \mathcal{V}_{HF}(jlk k') \psi_{nl}(k') = E_{nl} \psi_{nl}(k), \quad (34)$$

with  $m_{\text{eff}} = 2m(1 - 1/A)^{-1}$ . Here both  $k$  and  $k'$  are defined on an inversion symmetric contour  $L^+$  in the lower half complex  $k$ -plane, resulting in a closed integral equation. In order to solve this equation, the integral has to be discretized, and we finally end up with a complex symmetric matrix diagonalization problem, in analogy with Eq. (7). This procedure results in a self-consistent Gamow Hartree-Fock basis, which is complete within the discretization space, and includes bound, resonant and a finite set of non-resonant continuum states (see Ref. [19] for details about one-body Berggren completeness relations in momentum space).

Based on this approach, the single-particle Gamow Hartree-Fock states of the closed-shell  $^4\text{He}$  and  $^{16}\text{O}$  are calculated with a low-momentum nucleon-nucleon interaction constructed from the realistic  $\text{N}^3\text{LO}$  nucleon-nucleon interaction [34, 35]. For  $^{16}\text{O}$  we used the models spaces defined by  $\Lambda = 1.9, 2.0$  and  $2.1 \text{fm}^{-1}$ , and for  $^4\text{He}$  the models spaces defined by  $\Lambda = 1.8, 1.9$  and  $2.0 \text{fm}^{-1}$ .

Table I presents the neutron single-particle energies obtained with a  $^{16}\text{O}$  core. We note that holes states are in general overbound for all chosen cutoffs  $\Lambda$  and that the spin-orbit splitting between the  $p_{3/2}$  and  $p_{1/2}$  states is too large. The particle states are in better agreement with data and for all model spaces the  $d_{3/2}$  state is the only one which comes out as a resonance, in agreement with experiment. The spin-orbit spacing the  $d_{5/2}$  and  $d_{3/2}$  states is also fairly well reproduced. Fig. 2 shows the convergence of the  $0p_{3/2}$  and the  $0p_{1/2}$  spin-orbit partners in  $^{16}\text{O}$  with respect to the number of iterations in the self-consistent HF calculation.

Table II presents the calculated self-consistent neutron single-particle energies with respect to a  $^4\text{He}$  closed shell core. The calculated values for the  $p_{3/2}$  and the  $p_{1/2}$  energies are not so far from the experimental values. For a model space  $\Lambda = 1.8 \text{fm}^{-1}$ , the obtained width of the  $p_{3/2}$  resonance coincides with the experimental width  $0.648 \text{MeV}$ , while the calculated width of the  $p_{1/2}$  resonance ( $\sim 7.4 \text{MeV}$ ) is larger than the experimental value  $5.57 \text{MeV}$ . The spin-orbit splitting between the  $p_{3/2}$  and the  $p_{1/2}$  levels is fairly well reproduced, the experimental value is  $1.27 \text{MeV}$  [45] while our values vary from  $1.36$  to  $1.68 \text{MeV}$ . Noting that our calculations are done at the Hartree-Fock level, there is clearly room for improvements. However, although our results for hole states are overbound, we obtain a qualitatively correct spectrum. Higher-order corrections should improve the agreement with experiment, since  $2p - 1h$  and  $2h - 1p$  correlations provide additional binding and improved spin-orbit splittings for particle states.

Many-body calculations using a renormalized nucleon-nucleon interaction of the low-momentum type will unfortunately introduce a model space dependence in momentum space (see Tables I and II). The model space dependence can only be eliminated by introducing the corresponding three- and many-body forces which the low-momentum two-body interaction induces. In Gamow shell-model calculations, the inclusion of three-body forces is not feasible for the



TABLE I: HF calculation of single-particle energies in  $^{16}\text{O}$  using the low-momentum  $\text{N}^3\text{LO}$  nucleon-nucleon interaction for three different model spaces. The single-particle energies  $E$  are given in MeV for both real and imaginary parts. Experimental data are from Ref. [44].

	$\Lambda = 1.9 \text{ fm}^{-1}$		$\Lambda = 2 \text{ fm}^{-1}$		$\Lambda = 2.1 \text{ fm}^{-1}$		Expt.	
$lj$	Re[E]	Im[E]	Re[E]	Im[E]	Re[E]	Im[E]	Re[E]	Im[E]
$s_{1/2}$	-73.977	0.000	-68.496	0.000	-63.078	0.000	-44.000	0.000
$p_{3/2}$	-37.082	0.000	-33.824	0.000	-30.650	0.000	-21.840	0.000
$p_{1/2}$	-23.981	0.000	-21.749	0.000	-19.680	0.000	-15.664	0.000
$d_{5/2}$	-5.060	0.000	-3.810	0.000	-2.541	0.000	-4.143	0.000
$s_{1/2}$	-3.531	0.000	-2.556	0.000	-1.781	0.000	-3.273	0.000
$d_{3/2}$	5.189	-1.669	5.353	-1.928	5.419	-2.155	0.937	-0.048

TABLE II: Same as in Tab. I for  $^4\text{He}$ . Experimental data from Ref. [45].

	$\Lambda = 1.8\text{fm}^{-1}$		$\Lambda = 1.9\text{fm}^{-1}$		$\Lambda = 2.0\text{fm}^{-1}$		Expt.	
$lj$	Re[E]	Im[E]	Re[E]	Im[E]	Re[E]	Im[E]	Re[E]	Im[E]
$s_{1/2}$	-25.731	0.000	-24.541	0.000	-23.079	0.000	-20.578	0.000
$p_{3/2}$	0.819	-0.325	1.041	-0.479	1.287	-0.667	0.890	-0.324
$p_{1/2}$	2.497	-3.697	2.514	-3.777	2.648	-4.029	2.160	-2.785

moment. If one wants to minimize the effect from many-body forces, a better approach might be to use a  $G$ -matrix for nuclear matter as in Refs. [26, 39]. However, higher-order correlations such as  $2p-1h$  or  $2h-1p$  contributions are necessary in order to minimize the dependence on the starting energy and the chosen Fermi energy [39]. Whether the model space dependence of  $V_{\text{low-k}}$  can be softened by the inclusion of higher-order correlations such as  $2p-1h$  and  $2h-1p$  will be investigated in a future work. Furthermore, although the  $G$ -matrix carries an explicit starting energy dependence, this dependence is needed when one wants to compute for example spectral functions.

#### IV. MATRIX ELEMENTS OF REALISTIC NUCLEON-NUCLEON INTERACTION WITH A GAMOW HARTREE-FOCK BASIS

As discussed in the previous section, starting from matrix elements of the nucleon-nucleon interaction in the relative and center of mass system, one can obtain the corresponding matrix elements in the laboratory system through appropriate transformation coefficients, see for example Refs. [36, 37, 38] and the discussion in the previous section. This transformation proceeds through the definition of a two-particle state in the laboratory system using the vector bracket transformation. However, the latter is very complicated to handle in practical calculations beyond the Hartree-Fock level. One has also to face the problem of two-particle intermediate states not orthogonal to the incoming and outgoing states (see Eq. (29)). Another method is then needed in order to efficiently calculate effective nucleon-nucleon matrix elements in the complex  $k$ -plane and laboratory frame with a Gamow shell-model basis.

The renormalized nucleon-nucleon interaction in an arbitrary two-particle basis in the laboratory frame is given by

$$\langle ab|V_{\text{low-k}}|cd\rangle = \langle (n_a l_a j_a t_{z_a})(n_b l_b j_b t_{z_b})JT_z | V_{\text{low-k}} | (n_c l_c j_c t_{z_c})(n_d l_d j_d t_{z_d})JT_z \rangle. \quad (35)$$

The two-body state  $|ab\rangle$  is implicitly coupled to good angular momentum  $J$ . The labels  $n_{a\dots d}$  number all bound, resonant and discretized scattering states with orbital and angular momenta  $(l_{a\dots d}, j_{a\dots d})$ .

In order to efficiently calculate the matrix elements of Eq. (35), we introduce a two-particle harmonic oscillator basis completeness relation

$$\sum_{\alpha \leq \beta} |\alpha\beta\rangle \langle \alpha\beta| = \mathbb{1}, \quad (36)$$

where the sum is not restricted in the neutron-proton case. We introduce the greek single particle labels  $\alpha, \beta$  for the single-particle harmonic oscillator states in order to distinguish them from the latin single-particle labels  $a, b$  referring to Gamow states. The interaction can then be expressed in the complete basis of Eq. (36)

$$V_{\text{osc}} = \sum_{\alpha \leq \beta} \sum_{\gamma \leq \delta} |\alpha\beta\rangle \langle \alpha\beta| V_{\text{low-k}} |\gamma\delta\rangle \langle \gamma\delta|, \quad (37)$$

where the sums over two-particle harmonic oscillator states are infinite. The expansion coefficients

$$\langle \alpha\beta | V_{\text{low-}k} | \gamma\delta \rangle = \langle (n_\alpha l_\alpha j_\alpha t_{z_\alpha}) (n_\beta l_\beta j_\beta t_{z_\beta}) J T_z | V_{\text{low-}k} | (n_\gamma l_\gamma j_\gamma t_{z_\gamma}) (n_\delta l_\delta j_\delta t_{z_\delta}) J T_z \rangle, \quad (38)$$

represent the nucleon-nucleon interaction in an antisymmetrized two-particle harmonic oscillator basis, and may easily be calculated using the well known Moshinsky transformation coefficients, see for example Ref. [46] for expressions.

Matrix elements of Eq. (35) are calculated numerically in an arbitrary two-particle Gamow basis by truncating the completeness expansion of Eq. (37) up to  $N$  harmonic oscillator two-body states

$$\langle ab | V_{\text{osc}} | cd \rangle \approx \sum_{\alpha \leq \beta}^N \sum_{\gamma \leq \delta}^N \langle ab | \alpha\beta \rangle \langle \alpha\beta | V_{\text{low-}k} | \gamma\delta \rangle \langle \gamma\delta | cd \rangle. \quad (39)$$

The two-particle overlap integrals  $\langle ab | \alpha\beta \rangle$  read

$$\langle ab | \alpha\beta \rangle = \frac{\langle a | \alpha \rangle \langle b | \beta \rangle - (-1)^{J-j_\alpha-j_\beta} \langle a | \beta \rangle \langle b | \alpha \rangle}{\sqrt{(1+\delta_{ab})(1+\delta_{\alpha\beta})}} \quad (40)$$

for identical particles (proton-proton or neutron-neutron states) and

$$\langle ab | \alpha\beta \rangle = \langle a | \alpha \rangle \langle b | \beta \rangle \quad (41)$$

for the proton-neutron case. The one-body overlaps  $\langle a | \alpha \rangle$  are given by,

$$\langle a | \alpha \rangle = \int d\tau \tau^2 \varphi_a(\tau) R_\alpha(\tau) \delta_{l_\alpha l_\alpha} \delta_{j_\alpha j_\alpha} \delta_{t_\alpha t_\alpha}, \quad (42)$$

where  $\varphi_a$  is a Gamow single-particle state and  $R_\alpha$  is a harmonic oscillator wave function. The radial integral is either evaluated in momentum or position space, indicated by the integration variable  $\tau$ . The important point to notice is that the only numerical calculations involving Gamow states are the overlaps of Eq. (42). Hence, this expansion provides a simple analytical continuation of the nuclear interaction in the complex  $k$ -plane. More precisely, the expansion coefficients of Eq. (38) can always be calculated with real harmonic oscillator wave functions, and in the case of Gamow functions spanning a complex contour  $L^+$  (as in the momentum space representation), it is only the overlap integrals of Eq. (42) which are analytically continued in the complex plane. These one-body overlap integrals converge in all regions of the complex plane which are of physical importance, due to the gaussian fall off of the harmonic oscillator wave functions.

The convergence with the number of harmonic oscillator states  $N$  of the nuclear interaction expansion of Eq. (38) can however not be checked by considering the matrix elements of Eq. (39) when  $N \rightarrow +\infty$ . Indeed, they generally diverge when  $N \rightarrow +\infty$ , due to the long-range character of the nuclear interaction in laboratory coordinates. This reflects the fact that the convergence of the Gamow shell-model Hamiltonian with  $N$  is *weak*, because the representation of a Hamiltonian such as  $V_{\text{low-}k}$  in terms of a continuous Gamow basis is a distribution. Actually, only eigenvalues and eigenfunctions of the Gamow shell-model Hamiltonian converge with  $N$ , which will be shown in particular cases in Sec. V.

## V. GAMOW SHELL-MODEL CALCULATIONS OF ${}^6\text{HE}$ AND ${}^{18}\text{O}$ .

In Sec. III we constructed a self-consistent single-particle Gamow Hartree-Fock basis starting from a realistic renormalized nucleon-nucleon interaction. Ultimately this basis should be used to construct the effective interaction in a given model space and diagonalize the shell-model Hamiltonian. Using the harmonic oscillator expansion method of the nucleon-nucleon interaction, we have a practical way of constructing the effective interaction to be incorporated in Gamow shell-model calculations. It is our aim to investigate whether a finite truncation of the harmonic oscillator expansion given in Eq. (39) may yield converged energies and wave functions in Gamow shell-model calculations. As a first application we consider two nucleons moving outside a closed core. The Gamow shell-model Hamiltonian used reads

$$H(1, 2) = h_{\text{HF}}(1) + h_{\text{HF}}(2) + V_{\text{eff}}(1, 2), \quad (43)$$

where  $h_{\text{HF}}$  is the self-consistently derived single-particle Hartree-Fock potential and  $V_{\text{eff}}(1, 2)$  is the effective interaction acting between valence particles. In this work, all calculations are implemented up to first order in many-body perturbation theory, where the effective interaction is defined as

$$V_{\text{eff}}(1, 2) = V_{\text{low-}k}(1, 2) - \frac{\mathbf{k}_1 \cdot \mathbf{k}_2}{mA}. \quad (44)$$

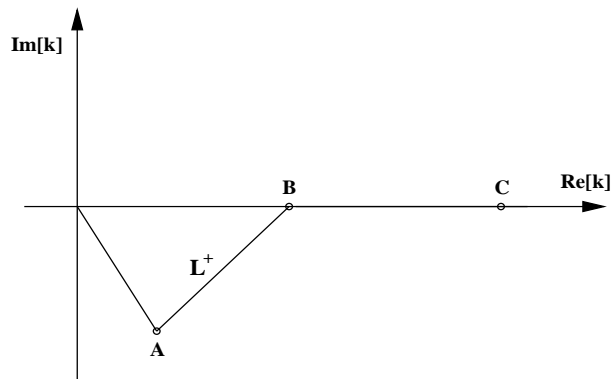


FIG. 3: Contour  $L^+$  in the complex  $k$ -plane used in construction of the single-particle Berggren basis. The contour is specified by the points  $A, B$  and  $C$  discussed in the text.

It should be noted that we utilize the harmonic oscillator expansion method only for the nucleon-nucleon interaction part, i.e.  $V_{\text{low-}k}(1, 2) \approx V_{\text{osc}}$ , while the center of mass correction term is treated exactly in the laboratory frame. The matrix elements of the center of mass term are given by

$$\begin{aligned} & \langle (n_a l_a j_a t_{z_a}) (n_b l_b j_b t_{z_b}) J T_z | \mathbf{k}_1 \cdot \mathbf{k}_2 | (n_c l_c j_c t_{z_c}) (n_d l_d j_d t_{z_d}) J T_z \rangle = \\ & -\hbar^2 (-1)^{j_c + j_a + J} \begin{Bmatrix} j_a & j_b & J \\ j_d & j_c & 1 \end{Bmatrix} \langle n_a l_a j_a || \nabla_1 || n_c l_c j_c \rangle \langle n_b l_b j_b || \nabla_2 || n_d l_d j_d \rangle, \end{aligned} \quad (45)$$

where the expression for the reduced matrix elements can be found in Ref. [46]. In our Gamow shell-model study of the two-particle valence systems with realistic interactions,  ${}^6\text{He}$  and  ${}^{18}\text{O}$ , a two-particle model space built from the  $s_{1/2}$ ,  $p_{3/2}$ ,  $p_{1/2}$ ,  $d_{5/2}$  and  $d_{3/2}$  single-particle states is used. Each combination of the quantum numbers  $lj$  consists of 25 single-particle orbitals, totalling 115 orbitals. The same integration contour  $L^+$  in the complex  $k$ -plane is used for all partial waves (see Fig. 3). In our  ${}^6\text{He}$  calculations the contour is defined with  $A = 0.28 - 0.12i \text{ fm}^{-1}$ ,  $B = 0.5 \text{ fm}^{-1}$  and  $C = 4 \text{ fm}^{-1}$ , and in our  ${}^{18}\text{O}$  calculations it is defined with  $A = 0.52 - 0.12i \text{ fm}^{-1}$ ,  $B = 0.64 \text{ fm}^{-1}$  and  $C = 4 \text{ fm}^{-1}$ . Using Gauss-Legendre quadrature, the discretization of  $L^+$  has been carried out with 5 points in the interval  $(0, A)$ , 7 points in the interval  $(A, B)$  and 13 points in the interval  $(B, C)$ . Convergence of the two-particle states with respect to the number of integration points has been checked. Our discretization of  $L^+$  yields a precision of the energy calculation better than 0.1 keV for all states considered. In the following discussion a model space defined by  $\Lambda = 1.9 \text{ fm}^{-1}$  is employed. The oscillator length is fixed at  $b = 2 \text{ fm}$ .

### A. ${}^6\text{He}$ results

Table III gives the convergence of the  $0_1^+$  ground state and the  $2_1^+$  excited state of  ${}^6\text{He}$  as functions of increasing number of nodes in the harmonic oscillator expansion of the interaction. A remarkable observation is that the  $0_1^+$  ground and the  $2_1^+$  excited states of  ${}^6\text{He}$  converge rather fast with respect to the number of harmonic oscillator functions, since  $n_{\text{max}} = 10$  is sufficient to reach convergence. Our calculations are comparable with the experimental values of  $-0.98 \text{ MeV}$  for the  $0^+$  ground state and  $1.8 - 0.06i \text{ MeV}$  for the  $2^+$  excited state in  ${}^6\text{He}$ . Especially the  $2^+$  excited state is well reproduced. A splitting of  $\sim 1.5 \text{ MeV}$  is obtained between the  $0^+$  ground state and the  $2^+$  excited state, to be compared with the experimental value of  $1.8 \text{ MeV}$ . The binding energy of the  $0^+$  ground-state may be improved by going beyond first order in many-body perturbation theory, as shown in for example Ref. [28]. The  $2p - 1h$  and  $1p - 2h$  diagrams may yield extra binding and improve spin-orbit splitting for the HF single-particle states of  ${}^4\text{He}$ . In addition, it is well-known that the two-body core-polarization contributions improve the spectroscopy of systems with two and more valence nucleons [28]. These findings agree also with Brueckner-Hartree-Fock calculations for oxygen isotopes, see for examples Ref. [47]. At first order in perturbation theory, the spectrum is very much compressed. The agreement with experiment is partly improved with the introduction of core-polarization contributions.

It can be concluded that the energies considered here for  ${}^6\text{He}$ , converge with respect to the number of harmonic oscillator functions in the expansion of the nucleon-nucleon interaction. However, this does not imply that other observables converge with the same speed, especially those which are sensitive to the tail of the wave function.

TABLE III: Convergence of the  $0_1^+$  and the  $2_1^+$  energies in  ${}^6\text{He}$  as functions of the number of harmonic oscillator nodes in the expansion of the realistic low-momentum  $\text{N}^3\text{LO}$  nucleon-nucleon interaction. The model space is given by  $\Lambda = 1.9 \text{ fm}^{-1}$ . The harmonic oscillator length is chosen at  $b = 2 \text{ fm}$ . Energies are given in units of MeV.

$n_{\text{max}}$	$J^\pi = 0_1^+$		$J^\pi = 2_1^+$	
	Re[E]	Im[E]	Re[E]	Im[E]
4	-0.4760	0.0000	0.9504	-0.0467
6	-0.4714	0.0000	0.9546	-0.0461
8	-0.4719	0.0000	0.9597	-0.0453
10	-0.4721	0.0000	0.9602	-0.0452
12	-0.4721	0.0000	0.9600	-0.0452
14	-0.4721	0.0000	0.9601	-0.0452
16	-0.4721	0.0000	0.9601	-0.0453
18	-0.4721	0.0000	0.9601	-0.0453
20	-0.4721	0.0000	0.9601	-0.0453

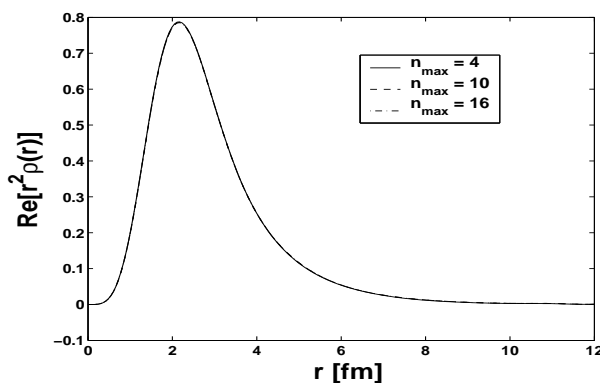


FIG. 4: Plot of the radial density of the  $0^+$  ground state of  ${}^6\text{He}$  for three different harmonic oscillator expansions with respectively  $n_{\text{max}} = 4, 10$  and  $16$ .

In order to investigate such a dependence, the single-particle radial density operator is considered for the  $0_1^+$  ground state in  ${}^6\text{He}$ . The single-particle radial density operator is given by

$$\hat{\rho} = \sum_i^N |r_i\rangle\langle r_i|, \quad (46)$$

where  $N$  is the total number of valence particles ( $N = 2$  for  ${}^6\text{He}$  in a  ${}^4\text{He}$  core). This operator measures the probability for either particle 1 or 2 is to be found at the position  $r_i$ . Fig. 4 shows plots of the diagonal part of  $\hat{\rho}$ , that is  $\rho(r = r_1 = r_2)$  for the  $0^+$  ground state of  ${}^6\text{He}$ , with  $n_{\text{max}} = 4, 10$  and  $16$  in the harmonic oscillator expansion of the nucleon-nucleon interaction. In Fig. 4 there is no observable difference between the  $n_{\text{max}} = 4, 10$  and  $16$  results. In Fig. 5 we examine the tail of the wave function. The densities obtained for  $n_{\text{max}} = 10$  and  $16$  are indistinguishable, while the  $n_{\text{max}} = 4$  displays a very small deviation from the converged results.

## B. ${}^{18}\text{O}$ results

Tab. IV gives the convergence of the  $0_1^+, 0_2^+, 4_1^+$  and  $4_2^+$  state energies and Tab. V the convergence of the  $2_1^+, 2_2^+, 2_3^+$  and  $2_4^+$  of  ${}^{18}\text{O}$ , as the number of nodes in the harmonic oscillator expansion increases. All of the states converge with a reasonable low number of harmonic oscillator functions  $n_{\text{max}} \sim 10$ . Our calculation of the  $0_1^+$  ground-state energy comes at  $-12.23\text{MeV}$  which is very close to the experimental value of  $-12.18\text{MeV}$ . The calculated splitting between the  $0_1^+$  ground-state and the  $0_2^+$  excited state is  $\sim 3.73\text{MeV}$  which is also very close to the experimental value  $3.63\text{MeV}$ . We are also able to predict that the first excited resonant state is the  $4_2^+$  state coming at energy  $-1.44 - 0.74i\text{MeV}$ , which is in agreement with experiment. However, we are not able to correctly describe

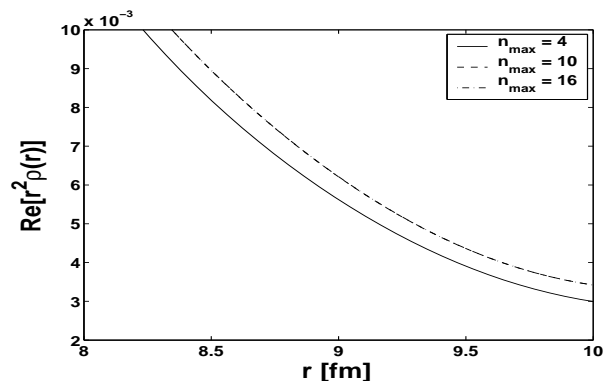


FIG. 5: Same as in Fig. 4, but for the radial interval  $8 \leq r \leq 10$ .

the splitting between the  $0_1^+, 2_1^+$  and the  $4_1^+$  states. In our calculations the  $0_1^+$  and  $2_1^+$  are almost degenerate. The discrepancy with experimental data is expected to be reduced by going beyond first order in perturbation theory, including contributions such as the core-polarization diagrams to the effective interaction. In Ref.[28], it was shown how the splitting of the  $0_1^+, 2_1^+$  and the  $4_1^+$  states of  $^{18}\text{O}$  is indeed improved by going to higher order in perturbation theory. In order to improve our Gamow shell-model calculations for  $^{18}\text{O}$  starting from realistic interactions, we must include higher order diagrams in the perturbation series for the nucleon self-energy and the effective interaction. This is a topic which will be followed up in the future.

TABLE IV: Convergence of the  $0_1^+, 0_2^+, 4_1^+$  and the  $4_2^+$  energies in  $^{18}\text{O}$  as functions of the number of harmonic oscillator nodes in the harmonic oscillator expansion. A model space defined by  $\Lambda = 1.9\text{fm}^{-1}$  was used. The harmonic oscillator length is fixed at  $b = 2$  fm. Energies are in units of MeV.

$n_{\text{max}}$	$J^\pi = 0_1^+$		$J^\pi = 0_2^+$		$J^\pi = 4_1^+$		$J^\pi = 4_2^+$	
	Re[E]	Im[E]	Re[E]	Im[E]	Re[E]	Im[E]	Re[E]	Im[E]
4	-12.225	0.000	-8.438	0.000	-11.0641	0.0000	-1.4373	-0.8275
6	-12.226	0.000	-8.498	0.000	-11.0907	0.0000	-1.4292	-0.7600
8	-12.228	0.000	-8.499	0.000	-11.0922	0.0000	-1.4380	-0.7405
10	-12.229	0.000	-8.499	0.000	-11.0921	0.0000	-1.4400	-0.7390
12	-12.228	0.000	-8.499	0.000	-11.0923	0.0000	-1.4393	-0.7401
14	-12.228	0.000	-8.499	0.000	-11.0923	0.0000	-1.4394	-0.7401
16	-12.228	0.000	-8.499	0.000	-11.0923	0.0000	-1.4394	-0.7401
18	-12.228	0.000	-8.499	0.000	-11.0923	0.0000	-1.4394	-0.7401
20	-12.228	0.000	-8.499	0.000	-11.0923	0.0000	-1.4394	-0.7401

## VI. EQUIVALENCE BETWEEN POSITION AND MOMENTUM SPACE REPRESENTATIONS

While the momentum representation of one-body Gamow states has been used in [19, 20] and here, the Gamow shell-model was first introduced employing a position space representation, see for example Refs. [14, 16]. A momentum space representation has however normally been preferred in constructions of effective interactions based on realistic nucleon-nucleon interaction models. There are several reasons for this. Realistic interactions are usually derived in  $k$ -space, so that plane wave expansions are the most natural bases. Moreover, in connection with Gamow shell-model calculations, the momentum space representation was meant to lead to a faster convergence with the number of discretized scattering states, as Gamow wave functions in momentum space are usually more localized compared to those in the coordinate representation. Moreover, the momentum space representation of the one-body Schrödinger equation is an integral equation in the general case, contrary to its integro-differential form in  $r$ -space, known to be much more difficult to solve. The necessity of imposing the asymptotics of the Gamow state in  $r$ -space was also thought to give rise to a slower convergence with the number of discretized scattering states. Finally, the use of complex scaling [48] to calculate two-body matrix elements in the position representation leads to extremely slow

TABLE V: Convergence of the  $2_1^+$ ,  $2_2^+$ ,  $2_3^+$  and the  $2_4^+$  energies in  $^{18}\text{O}$  as functions of the number of harmonic oscillator nodes in the harmonic oscillator expansion. A model space defined by  $\Lambda = 1.9\text{fm}^{-1}$  was used. The harmonic oscillator length is fixed at  $b = 2$  fm. Energies are in units of MeV.

$n_{\text{max}}$	$J^\pi = 2_1^+$		$J^\pi = 2_2^+$		$J^\pi = 2_3^+$		$J^\pi = 2_4^+$	
	Re[E]	Im[E]	Re[E]	Im[E]	Re[E]	Im[E]	Re[E]	Im[E]
4	-12.1398	0.0000	-10.0488	0.0000	-0.0772	-1.4465	1.1632	-1.4478
6	-12.1465	0.0000	-10.0830	0.0000	-0.1321	-1.3038	1.1628	-1.5059
8	-12.1452	0.0000	-10.0853	0.0000	-0.1539	-1.2929	1.1836	-1.5346
10	-12.1450	0.0000	-10.0857	0.0000	-0.1595	-1.2922	1.1807	-1.5331
12	-12.1453	0.0000	-10.0858	0.0000	-0.1570	-1.2938	1.1820	-1.5343
14	-12.1453	0.0000	-10.0858	0.0000	-0.1571	-1.2938	1.1821	-1.5342
16	-12.1453	0.0000	-10.0858	0.0000	-0.1573	-1.2936	1.1822	-1.5342
18	-12.1453	0.0000	-10.0858	0.0000	-0.1573	-1.2936	1.1822	-1.5342
20	-12.1453	0.0000	-10.0858	0.0000	-0.1573	-1.2936	1.1822	-1.5342

calculations and cannot even regularize a large class of infinite matrix elements occurring in long-range interactions. It was this last nuisance which motivated the use of surface-peaked interactions in position space calculations, namely the Surface Delta Interaction (SDI) [14, 15] and the Surface Gaussian Interaction (SGI) [11, 12]. One will see however that both representations are in fact equivalent theoretically but also numerically, where the computational cost to obtain a given precision is comparable in both cases. The main point is that the possibility to use the harmonic oscillator expansion method of Sec. IV removes all the problems previously encountered with both representations.

In order to obtain a self-consistent Gamow Hartree-Fock basis in position space, one has to solve the one-body integro-differential Schrödinger equation

$$\frac{\hbar^2}{m_{\text{eff}}}\varphi''_{nlj}(r) + \int_0^{+\infty} dr' \mathcal{V}_{HF}(jlr'r')\varphi_{nlj}(r') = E_{nl}\varphi_{nlj}(r), \quad (47)$$

where  $\mathcal{V}_{HF}(jlr'r')$  is the self-consistent HF potential given in Eq. (32). The wave function  $|\varphi_{nlj}\rangle$  has to exhibit a pure outgoing wave function behavior for bound and resonant states for  $r \rightarrow +\infty$ , whereas it has both incoming and outgoing components if it is a scattering state. In the last case,  $n$  must be understood as representing its wave number  $k$ . Even though it is an integro-differential equation, it can be solved with standard methods with the use of locally equivalent potentials [49], so that its integration has the same complexity as differential equations occurring with purely local potentials. This generates a self-consistent procedure, as the locally equivalent potential depends on the state that it generates. This is of no importance in practical situations, as the integrated potential will be non-local in  $r$ -space only if it is a HF potential generated by a finite-range interaction. As HF potentials have to be solved self-consistently, no numerical overhead can occur. The slow convergence noted in Ref. [14] was due only to the use of the trapezoidal rule to discretized the non-resonant continuum. With the use of the Gauss-Legendre integration, as performed in  $k$ -space calculations from the beginning, results have improved dramatically in  $r$ -space calculations, reaching  $k$ -space calculations quality [50].

In fact, the fundamental difference between the  $r$  and the  $k$  representations for Gamow shell-model applications lies in their different discretization schemes. In  $k$ -space, it is the Bessel completeness relation of Eq. (6) which is discretized. The  $|\psi_{nlj}\rangle$  states are then obtained by diagonalization of  $\mathcal{V}_{HF}(jlk'k')$  in the discretized Fourier-Bessel basis space. They will be denoted as  $|\psi_{nl}\rangle^{D_k}$ . In  $r$ -space, it is the completeness relation spanned by the  $|\varphi_{nl}\rangle$  states themselves which is discretized. Indeed, one has :

$$\sum_{n \in (b,d)} |\varphi_{nl}\rangle\langle\varphi_{nl}| + \int_{L_+} |\varphi_{kl}\rangle\langle\varphi_{kl}| dk = \mathbb{1} \quad (48)$$

$$\sum_{i=1}^N w_n |\varphi_{nl}\rangle\langle\varphi_{nl}| \simeq \mathbb{1}, \quad (49)$$

where  $n \in (b, d)$  means that one sums over all bound ( $b$ ) and decaying ( $d$ ) states above the contour  $L_+$ . The first completeness relation, exact, becomes the second discretized completeness relation, approximate, where  $w_n$  is 1 for bound and resonant states, and the Gauss-Legendre weight for scattering states. As a consequence, the  $|\varphi_{nl}\rangle$  states of  $r$ -space, that we label  $|\varphi_{nl}\rangle^{D_r}$  are exact up to numerical precision, since they come from a direct integration of the Schrödinger equation. Approximations arise only from their discrete and finite number in Eq. (49). The corresponding

$|\psi_{nl}\rangle^{D_k}$  states have to be approximate, as they are generated by a finite number of Bessel basis states, meaning that there are not enough frequencies to expand them exactly. As a consequence, one has  $|\psi_{nl}\rangle^{D_k} \rightarrow |\psi_{nl}\rangle^{D_r}$  only at the continuum limit, that is for  $N \rightarrow +\infty$ .

This difference may appear for observables that depend on large values of  $r$  or  $k$ , such as particle densities at large  $r$  or momentum densities at large values of  $k$ . But this is of no importance as discretization effects become preponderant in these regions, and may thereby most likely lead to numerically unstable results.

Consequently, both representations can be used in shell-model problems without any loss of precision. The remaining question of the method to handle two-body matrix elements in purely numerical bases has been answered in Sec. IV with the use of harmonic oscillator expansions. One has seen in the latter section that the only numerical calculations involving Gamow states are the overlaps between Gamow and harmonic oscillator states of Eq. (42), which are obviously fast numerically. The Gaussian decrease of harmonic oscillator states in momentum or position representation allows a very accurate implementation of overlaps in both representations. Hence, the implementation of the Gamow shell-model matrix becomes very similar from one representation to another.

The Coulomb interaction, not considered in this paper, may however generate difficulties in the momentum representation. Its infinite range character can indeed be treated exactly in the  $r$ -representation at the basis level through the use of Coulomb wave functions, whereas approximations have to be performed in  $k$ -space calculation as the Fourier-Bessel transform of the Coulomb interaction does not exist. The use of the harmonic oscillator expansion method may be indeed slowly converging for its low multipoles. This question will have to be answered with Gamow shell-model calculations of nuclei close to the proton drip-line.

## VII. CONCLUSION AND FUTURE PERSPECTIVES

In this paper we have presented a calculational algorithm which can be used to obtain a self-consistent single-particle basis in the complex energy plane, starting from a renormalized and realistic nucleon-nucleon interaction. In this work we used the simplest possible approximation to the nucleon self-energy, including the Hartree-Fock diagram only in order to demonstrate the feasibility of our method. With our approach we studied the single-particle spectra of  ${}^4\text{He}$  and  ${}^{16}\text{O}$ . For  ${}^4\text{He}$  we found that both the  $p_{3/2}$  and the  $p_{1/2}$  states appeared as resonances. Their widths are in fair agreement with experiment. For  ${}^{16}\text{O}$  we found the hole states to be largely overbound, while the  $s_{1/2}$  and  $d_{5/2}$  particle states agree well with the experimental values. The  $d_{3/2}$  states comes out as a resonance, in agreement with experiment although our width is larger than the experimental value. Higher order corrections such as  $2p - 1h$  and  $1h - 2p$  contributions may improve the agreement with experiment, in particular the spin-orbit splittings for the hole states, and will be included in future self-energy calculations.

With the Gamow Hartree-Fock single-particle basis, derived from realistic interactions, the problem of representing the nucleon-nucleon interaction in the derived basis comes to the fore. As the nucleon-nucleon interaction is typically given in momentum space, a transformation from the relative and center of mass frame to the laboratory frame involves mathematical functions which are not easy to continue analytically in the complex  $k$ -plane. To that end, we investigated whether a method based on an expansion of the nucleon-nucleon interaction as function of a finite set of harmonic oscillator functions could be a promising route. This expansion allows for a straightforward calculation of matrix elements in the laboratory frame for any Gamow basis. The harmonic oscillator functions are indeed very flexible in both position and momentum space, and the analytic continuation of the two-body interaction in the complex plane turns out to be very easy to implement from both a theoretical and a numerical point of view. With this method, we have shown that for the example of the  ${}^6\text{He}$  and  ${}^{18}\text{O}$  nuclei, all states converge with a low number of harmonic oscillator functions in the expansion of the interaction. This method offers also a practical way of calculating higher order diagrams in many-body perturbation theory. There are diagrams which enter for example the definition of the self-energy and two or three-body effective interactions. In particular, this method provides a solution to the problem of non-orthogonal intermediate particle states, a problem which arises when one uses the vector brackets. Utilizing the harmonic oscillator expansion of the interaction, we ensure that all intermediate states are orthogonal in all diagrams beyond first order in many-body perturbation theory. However, the renormalization of the Coulomb interaction and the two-body center of mass contribution need further considerations.

The procedure outlined in this work allows for several interesting applications related to the study of weakly bound and unbound nuclei along the driplines. Of particular interest is the possibility to apply our approach within the framework of the coupled-cluster method, see for example Refs. [54, 55, 56, 57, 58, 59]. The coupled-cluster approach is a promising candidate for the development of practical methods for fully microscopic *ab initio* studies of nuclei. The coupled-cluster methods are capable of providing a precise description of many-particle correlation effects at relatively low computer costs, when compared to shell-model or configuration interaction techniques aimed at similar accuracies. In approaches such as the coupled cluster, an extension to the complex energy plane is in principle possible. Coupled-cluster calculations starting with a HF basis in the complex plane, along with the inclusion of

realistic interactions, are planned in near future. Then, it might be possible to perform coupled-cluster calculations of states with a multi-particle resonant structure starting with a realistic interaction.

### Acknowledgments

Discussions with Jimmy Rotureau are gratefully acknowledged. This work was supported in part by the U.S. Department of Energy under Contracts Nos. DE-FG02-96ER40963 (University of Tennessee), DE-FG05-87ER40361 (Joint Institute for Heavy Ion Research), and the Research Council of Norway (Supercomputing grant NN2977K). Oak Ridge National Laboratory is managed by UT-Battelle for the U.S. Department of Energy under Contract No. DE-AC05-00OR22725.

- 
- [1] V. Zhukov, B. Danilin, D. Fedorov, J. Bang, I. Thompson, and J. Vaagen, *Phys. Rep.* **231**, 151 (1993).
  - [2] A. Volya and V. Zelevinsky, *Phys. Rev. C* **67**, 054322 (2003).
  - [3] A. Volya and V. Zelevinsky, *Phys. Rev. Lett.* **94**, 052501 (2005).
  - [4] A. Volya and V. Zelevinsky, preprint nucl-th/0509051.
  - [5] I. Rotter, *Rep. Prog. Phys.* **54**, 635 (1991).
  - [6] I. Rotter, *Phys. Rev. E* **64**, 036213 (2001).
  - [7] K. Bennaceur, F. Nowacki, J. Okołowicz, and M. Płoszajczak, *Nucl. Phys. A* **651**, 289 (1999).
  - [8] K. Bennaceur, F. Nowacki, J. Okołowicz, and M. Płoszajczak, *Nucl. Phys. A* **671**, 203 (2000).
  - [9] J. Okołowicz, M. Płoszajczak, and I. Rotter, *Phys. Rep.* **374**, 271 (2003).
  - [10] J. Rotureau, J. Okołowicz, and M. Płoszajczak, *Phys. Rev. Lett.* **95**, 042503 (2005).
  - [11] N. Michel, W. Nazarewicz, and M. Płoszajczak, *Phys. Rev. C* **70**, 064313 (2004).
  - [12] N. Michel, W. Nazarewicz, M. Płoszajczak, and J. Rotureau, *Rev. Mex. Fis.* **50 Suppl. 2**, 74 (2004).
  - [13] J. Dobaczewski, N. Michel, W. Nazarewicz, M. Płoszajczak, and M. V. Stoitsov, nucl-th/0401034 (2004).
  - [14] N. Michel, W. Nazarewicz, M. Płoszajczak, and K. Bennaceur, *Phys. Rev. Lett.* **89**, 042502 (2002).
  - [15] N. Michel, W. Nazarewicz, M. Płoszajczak, and J. Okołowicz, *Phys. Rev. C* **67**, 054311 (2003).
  - [16] R. Id Betan, R. J. Liotta, N. Sandulescu, and T. Vertse, *Phys. Rev. Lett.* **89**, 042501 (2002).
  - [17] R. Id Betan, R. J. Liotta, N. Sandulescu, and T. Vertse, *Phys. Rev. C* **67**, 014322 (2003).
  - [18] R. Id Betan, R. J. Liotta, N. Sandulescu, and T. Vertse, *Phys. Lett. B* **584**, 48 (2004).
  - [19] G. Hagen, J. S. Vaagen, and M. Hjorth-Jensen, *J. Phys. A: Math. Gen.* **37**, 8991 (2004).
  - [20] G. Hagen, M. Hjorth-Jensen, and J. Vaagen, *Phys. Rev. C* **71**, 044314 (2005).
  - [21] T. Berggren, *Nucl. Phys. A* **109**, 265 (1968).
  - [22] T. Berggren, *Nucl. Phys. A* **169**, 353 (1971).
  - [23] T. Berggren, *Phys. Lett. B* **73**, 389 (1978).
  - [24] T. Berggren, *Phys. Lett. B* **373**, 1 (1996).
  - [25] P. Lind, *Phys. Rev. C* **47**, 1903 (1993).
  - [26] M. Borromeo, D. Bonatsos, H. Müther, and A. Polls, *Nucl. Phys. A* **539**, 189 (1992).
  - [27] D. Bonatsos and H. Müther, *Nucl. Phys. A* **496**, 23 (1989).
  - [28] M. Hjorth-Jensen, T. T. S. Kuo, and E. Osnes, *Phys. Rep.* **261**, 125 (1995).
  - [29] S. K. Bogner, T. T. S. Kuo, and A. Schwenk, *Phys. Rep.* **386**, 1 (2003).
  - [30] S. Fujii, E. Epelbaum, H. Kamada, R. Okamoto, K. Suzuki, and W. Glöckle, *Phys. Rev. C* **70**, 024003 (2004).
  - [31] S. Fujii, R. Okamoto, and K. Suzuki, *Phys. Rev. C* **71**, 054301 (2004).
  - [32] S. Bogner, T. T. S. Kuo, L. Coraggio, A. Covello, and N. Itaco, *Phys. Rev. C* **65**, 051301 (2002).
  - [33] A. Nogga, S. K. Bogner, and A. Schwenk, *Phys. Rev. C* **70**, 061002 (2004).
  - [34] D. R. Entem and R. Machleidt, *Phys. Lett. B* **524**, 93 (2002).
  - [35] D. R. Entem and R. Machleidt, *Phys. Rev. C* **68**, 041001 (2003).
  - [36] R. Balian and E. Brezin, *Nuovo Cim.* **61**, 403 (1969).
  - [37] C. W. Wong and D. M. Clement, *Nucl. Phys. A* **183**, 210 (1972).
  - [38] C. L. Kung, T. T. S. Kuo, and K. F. Ratchiff, *Phys. Rev. C* **19**, 1063 (1979).
  - [39] I. Vidaña, A. Polls, A. Ramos, and M. Hjorth-Jensen, *Nucl. Phys. A* **644**, 201 (1998).
  - [40] K. Suzuki, *Progr.Theor.Phys.* **68**, 246 (1982).
  - [41] K. Suzuki and R. Okamoto, *Progr.Theor.Phys.* **93**, 905 (1995).
  - [42] S. Okubo, *Prog. Theor. Phys.* **12**, 603 (1954).
  - [43] J. D. Holt, T. T. S. Kuo, and G. E. Brown, *Phys. Rev. C* **69**, 034329 (2004).
  - [44] R. B. Firestone, V. S. Shirley, C. M. Baglin, S. Y. F. Chu, and J. Zipkin, *Table of Isotopes, Eighth Edition* (Wiley Interscience, New York) (1996).
  - [45] D. R. Tilley, C. M. Chevesa, J. L. Godwin, G. M. Hale, H. M. Hofmann, J. H. Kelley, C. G. Sheu, and H. R. Weller, *NPA* **708**, 3 (2002).



- [46] R. D. Lawson, *Theory of the Nuclear Shell Model* (Clarendon Press, 1980).
- [47] M. Hjorth-Jensen, E. Osnes, H. Müther, and K. W. Schmid, *Phys. Lett. B* **248**, 243 (1990).
- [48] B. Gyarmati and T. Vertse, *Nucl. Phys. A* **160**, 523 (1971).
- [49] D. Vautherin and M. Vénéroni, *Phys. Lett. B* **25**, 175 (1957).
- [50] N. Michel, W. Nazarewicz, M. Płoszajczak, and J. Rotureau, nucl-th/0601055, submitted to *Phys. Rev. Lett.* (2006).
- [51] J. P. Elliott and T. H. R. Skyrme, *Proc. Roy. Soc. A (London)* **232**, 561 (1955).
- [52] P. Navrátil, G. P. Kamuntavicius, and B. R. Barrett, *Phys. Rev. C* **61**, 044001 (2000).
- [53] N. Michel, W. Nazarewicz, M. Płoszajczak, and J. Rotureau, unpublished (2006).
- [54] F. Coester, *Nucl. Phys.* **7**, 421 (1958).
- [55] F. Coester and H. Kümmel, *Nucl. Phys.* **17**, 477 (1960).
- [56] J. Čížek, *J. Chem. Phys.* **45**, 4256 (1966); *Adv. Chem. Phys.* **14**, 35 (1969).
- [57] J. Čížek and J. Paldus, *Int. J. Quantum Chem.* **5**, 359 (1971).
- [58] K. Kowalski, D. J. Dean, M. Hjorth-Jensen, T. Papenbrock, and P. Piecuch, *Phys. Rev. Lett.* **92**, 132501 (2004).
- [59] M. Włoch, D. J. Dean, J. R. Gour, M. Hjorth-Jensen, K. Kowalski, T. Papenbrock, and P. Piecuch, *Phys. Rev. Lett.* **94**, 132501 (2005).